HYDRATE BLOCKAGE POTENTIAL IN AN OIL-DOMINATED SYSTEM STUDIED USING A FOUR INCH FLOW LOOP

John Boxall, Simon Davies, Joe Nicholas, Carolyn Koh and E. Dendy Sloan [*]
Center for Hydrate Research
Department of Chemical Engineering
Colorado School of Mines
1600 Illinois St, Golden, CO
USA

Doug Turner, Larry Talley
ExxonMobil Upstream Research Center
Houston, TX,
USA

ABSTRACT

An understanding of the blockage potential for an oil dominated system is an important step in moving from hydrate prevention to hydrate management. To better understand this problem a series of experiments were performed by varying the water cut, fluid velocity, and gas-liquid volume fraction using the ExxonMobil (XoM) flow loop in Houston, Texas, USA.

The XoM large loop is a three pass, four inch internal diameter flow loop with a sliding vane pump capable of generating liquid velocities of up to 4 m/s. The systems that were studied include a range of water cuts from 5%-50% in a light crude oil (Conroe crude) and a gas phase of either pure methane for sI or 75% methane and 25% ethane which has sII as the thermodynamically stable phase.

The results are compared with the hydrate plug prediction tool, CSMHyK, integrated into the multiphase flow simulator OLGA5[®]. The comparison between the model and the flow loop results serve as a basis for improving hydrate formation and plug prediction. In addition, the experimental variables that promote plug formation in the flow loop and how these may translate into the field are discussed.

Keywords: flow assurance, hydrate kinetics, hydrate transportability, flow loops, OLGA

NOMENCLATURE

k'_f observed formation rate constant
k_B intrinsic kinetics rate constant
u formation rate constant adjustment
ω flow loop pump speed
ϕ_g gas volume fraction
ϕ_{wc} water cut
η oil viscosity

INTRODUCTION

One current state-of-the-art model for hydrate plug formation CSMHyK [1] (the Colorado School of Mines Hydrate Kinetics model) has recently been incorporated into the OLGA multiphase flow simulator and provides an estimate of where and approximately when a hydrate plug may form. Lack of oil pipeline hydrate plug formation data led to a need for an alternative means of verifying

[*] Corresponding author: Phone: +1 303 273 3723 Fax +1 303 273 3730 E-mail: esloan@mines.edu

the hydrate formation model. Flow loop experiments have often been seen as a necessary method towards understanding hydrate plug formation in oil dominated systems. A method of modeling flow loop experiments using the transient multiphase flow simulator OLGA5[®], as a verification tool for the hydrate plug formation model CSMHyK, has been implemented. This paper presents flow loop results that have been used to verify the hydrate formation model. Results from hydrate formation experiments investigating the effect of the experimental variables on the plugging behavior of hydrate formation from water-in-oil emulsions are also presented.

Two major aspects of the hydrate flow loop experiments are discussed. The first is the dependent variable - namely increased flow loop pressure drop (ΔP) due to hydrate formation and the translation of ΔP results to a hypothesis of transportability for hydrate slurries. The second aspect is the hydrate formation rate and the comparison of the experimental data with the hydrate kinetic model simulations using CSMHyK-OLGA.

Flow Loop Description

The flow loop experiments were performed using the ExxonMobil flow loop at the Friendswood facility in Houston, Texas. The flow loop (Figure 1) is a triple pass loop which consists of a 3.8 inch diameter pipe, 312 feet long. The loop flow impeller is a custom-made sliding vane pump. The loop is enclosed in an environmentally controlled room, except for a short outdoor extension containing a dipped section with a 3.4 foot down/up section and a 4.75 straight section along the bottom of the dip. View ports are located just before and at the bottom of the dip section. An FBRM[®] particle size analyzer is installed in the up-flow portion of the dip section. This location ensured effective sampling of the cross-section of all fluids in the loop. Gas pressure in the loop was kept constant via a gas accumulator, since gas was consumed during hydrate formation. The gas accumulator was piston driven via a hydraulic high pressure unit (HPU) to maintain constant loop pressure. Gas was circulated from the loop, through a coil attached to the moving piston, and back into the loop to maintain a more constant gas composition.

Another recent addition to the flow loop was the mass flow and density meter.
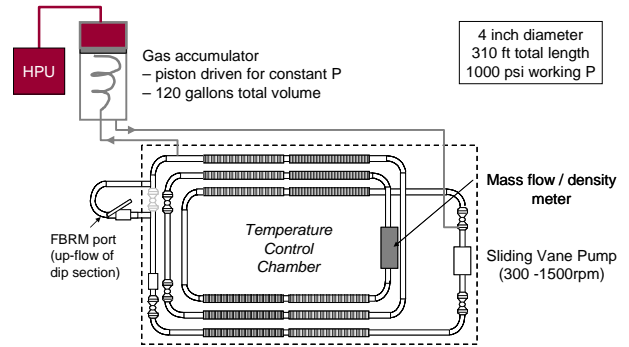

Figure 1. Schematic of the ExxonMobil flow loop with FBRM and mass flow meter

CMSHyK Model Description

CSMHyK is a plug-in module for the OLGA5[®] (SPT Group) multiphase flow simulator. Researchers at CSM have been developing the module in cooperation with SPT Group since 2003. The model predicts the rate of hydrate formation using a first-order rate equation based on the thermal driving force. The rate equation (Equation 1) was originally proposed by Vysniauskas and Bishnoi [2] in the absence of mass and heat transfer limitations.

$$-\frac{dm_{gas}}{dt} = k_B A_S (\Delta T) \qquad (1),$$

where m_{gas} is the gas mass, k_B is the reaction rate constant, A_s is the surface area of the interface of the aqueous phase, and ΔT is the subcooling.

The current model assumes that hydrate particles convert directly from emulsified water droplets. Nucleation is assumed to occur instantaneously at a sub-cooling of 6.5°F, a default parameter proposed by Matthews [3], but also a user-adjustable parameter. Once hydrate is formed, the model assumes that these particles remain in the oil phase. The change in relative viscosity of this phase is then found from the Camargo and Palermo [4] correlation for steady state slurry flow. A more detailed overview of the current CSMHyK module and its integration into OLGA[®] can be found in our previous paper [5]. When comparing the model with the flow loop experiments two adjustable parameters are used:

(1) the hydrate nucleation sub-cooling and (2) the fitted multiplier of the kinetic constant , u, given in Equation 2.

$$k'_f = u \ k_B$$

(2).

where u = the fitting parameter, and k_B = the intrinsic kinetic rate constant fitted to Bishnoi's data [2].

Modelling a Flow Loop using OLGA

The basic template model for modeling a flow loop in OLGA required an inlet, split, merge, and outlet node (Figure 2). The flow loop was the pipeline between the split and merge nodes. A volume pump provided the loop with circular flow. The constant volume and constant pressure flow loop scenarios required slightly different modeling in OLGA5®. For a constant volume flow loop experiment, a closed valve on either side of the dummy pipelines isolated the flow loop. For the constant pressure case, an additional terminal node was used to add or remove gas from the flow loop, to maintain pressure. The dummy branch attached to this node was vertical and transmitted the specified pressure to the loop without removing liquid from the system.
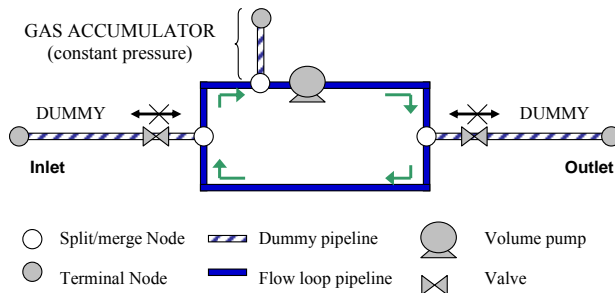

Figure 2. OLGA5® flow loop simulation template

Experimental Variables

Three separate long-term visits to the ExxonMobil flow loop have resulted in the tests discussed here (Test Matrices I, II, and III). Water cut (ϕ_{wc}), motor speed (ω), and gas fraction (ϕ_g), were varied in the experiments during the first visit (Test Matrix I). A continuation of the Test Matrix I was performed for Test Matrix II, adding two additional experimental variables, viscosity and super-saturation (pressure) or the driving force for

hydrate formation. Table 1 gives the experimental variables examined in the Test Matrix I and II flow loop experiments and the values of each variable.

Table 1. Matrix for high and low parameters for Test Matrix I and II flow loop experiments.

	Pump Speed (ω)	Gas Volume Fraction (ϕ_g)	Water Cut (ϕ_{wc})	Pressure (P) [psig]	Oil viscosity (η) [cP]
+	550	5%	35%	950	100
−	300	46%	5%	735	5

The two oils used were Conroe crude and a blend of Conroe with a distillate product oil, Brightstock. The Conroe crude is a light crude oil with a specific gravity of 0.84 and a very low asphaltene content (0.31wt%). Brightstock is a distillate product mineral oil with a specific gravity of 0.90 and no asphaltene content. Conroe crude was used as the low viscosity fluid (5 cP @40°F) and a 50:50 volume mixture of Brightstock and Conroe was used as the high viscosity fluid (~100 cP). The driving force for hydrate formation was adjusted using the flow loop pressure; with the gas phase being pure methane for sI hydrates. The operating temperature for all experiments was 40°F. A factorial test matrix was designed to identify variables affecting hydrate growth rate and agglomeration; as well as to determine variable values for future experiments.

For the Test Matrix I and II experiments the maximum pump speed was limited to 550 rpm; however for the third set of experiments (Test Matrix III) this speed was extended to 1500 rpm, so that experiments at much higher flow rates (600, 900 and 1400 rpm which correspond to multiphase velocities of 4.7, 7.6, 12.3 ft/s) were run during Test Matrix III. The other experimental variables investigated during Test Matrix III were intermediate liquid volume fractions (70% and 90% liquid loading compared to 54% and 95% in the past) and intermediate and high water cuts (25%, 37.5%, 50% water cuts compared to 5% and 35% in the past). Also, the gas phase was changed for these experiments from pure methane gas to a 75:25 mol% methane:ethane mixture, which forms sII hydrate as its thermodynamically stable phase for the temperatures-pressures of interest.

Table 2. Experimental parameters for Test Matrix III flow loop experiments.

Pump Speed (ω)	Gas Volume Fraction (φ_g)	Water Cut (φ_wc)
1400	10%	50%
900	30%	37.5%
600		25%

RESULTS – HYDRATE FORMATION, FLOW LOOP PRESSURE DROP AND PLUGGING TENDENCY

High Liquid Loading – 90% Liquid

Figure 3 shows the hydrate formation in terms of conversion of the available water for three different pump speeds. The result shows that hydrate formation decreases after initially fast conversion. This observation supports a shell growth model limited by mass transfer through an initial hydrate shell. There does appear to be some dependence on the pump speed were there is greater overall conversion for the higher pump speeds, although the initial formation rates are very similar for all three.
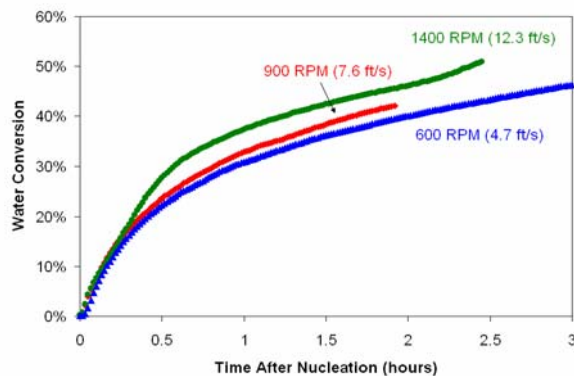
Figure 3. Hydrate formation with 90% liquid loading, 25% water cut, and Conroe crude oil (75% methane, 25% ethane gas)

Figure 4 shows the flow loop pressure drop as a function of the hydrate volume fraction in the slurry. With up to 15% hydrate volume fraction (in these experiments) there is very little to no increase in flow loop pressure drop. This observation indicates that under the given flow conditions (moderate to high velocity and very high liquid volume fraction) the droplets are
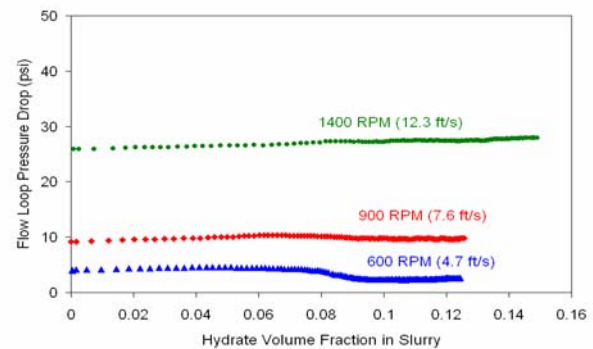
Figure 4. Flow loop pressure drop versus hydrate volume fraction with 90% liquid loading, 25% water cut, and Conroe crude oil (75% methane, 25% ethane gas)

Intermediate Liquid Loading – 70% Liquid

Figure 5 shows hydrate formation (in terms of water conversion) for two different pump speeds (900 and 1400 rpm) and two different water cuts (37.5% and 50%) with a 70% liquid volume fraction (dead oil) flow loop loading. Like the 90% liquid loading case there does not appear to be a very significant effect of the pump speed on the initial formation rate but the results do show that the lower water cut does result in a higher overall hydrate conversion. The 37.5% water cut case forms hydrate at a steady (faster) rate before the flow loop pressure drop limit forces the experiment to be stopped (as can be seen in Figure 6). For the 50% water cut case, the formation rate decreases significantly after approximately 30% conversion of the water to hydrate (Figure 5).
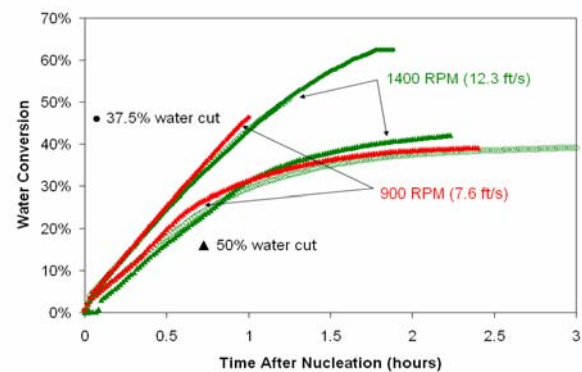
Figure 5. Hydrate formation with 70% liquid loading and Conroe crude oil (75% methane, 25% ethane gas phase) – open symbols = repeat

Figure 6 and 7 give the flow loop pressure drop plotted versus the hydrate volume fraction and correspond to the formation results shown in Figure 5. These results indicate that at the lower pump speed (Figure 6 – 900 rpm) both water cuts *plugged* the flow loop. In this case *plugged* refers to the 50 psi pump pressure drop safety cut off. At the higher pump speed the increase in pressure drop to an eventual *plug* is only seen in the lower water cut (Figure 7 – 1400 rpm).
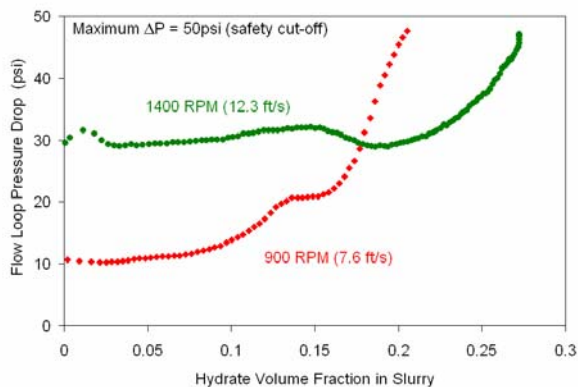

Figure 6. Flow loop pressure drop versus hydrate volume fraction with 70% liquid loading, 37.5% water cut, and Conroe crude oil (75% methane, 25% ethane gas phase)
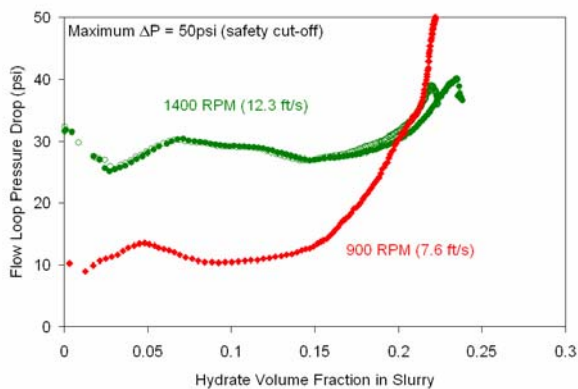

Figure 7. Flow loop pressure drop versus hydrate volume fraction with 70% liquid loading, 50% water cut, and Conroe crude oil (75% methane, 25% ethane gas phase) – open symbols = repeat

One hypothesis for these observations is at the higher shear/higher water content, the slurry is transformed into a *pumpable slurry* or *slush*, whereas in plugging cases at lower shear/lower water content the slurry has agglomerated and deposited in the flow loop. Hydrate formation in these cases was often limited by the experiment, as the pump safety cut-off was reached before formation ended. The observed extent of hydrate formation ranged from 30-60% conversion of the water (12-18% hydrate volume fraction).

Low Liquid Loading – 54% Liquid

Figure 8 shows hydrate formation for two different pump speeds (300 and 550 rpm or 1.9 and 4.3 ft/s) with a gas volume of just under 50%. This gas volume was the highest achievable void fraction for the flow loop, due to the limitations of the pump. The data plotted represent two repeat runs for each pump speed and show the least repeatability out of the different liquid loadings.
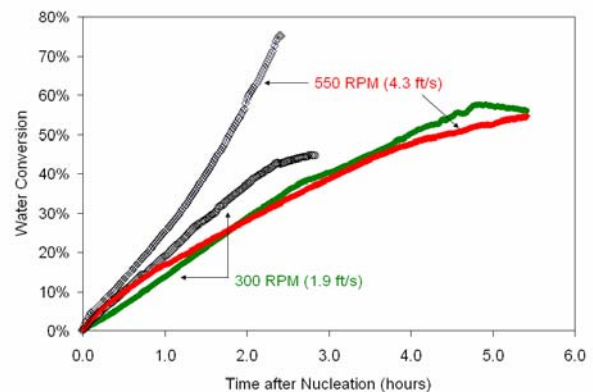

Figure 8. Hydrate formation with 54% liquid loading, 35% water cut and Conroe crude oil (100% methane gas) – open symbols = repeat

Figure 9 shows the flow loop pressure drop versus the hydrate volume fraction in the slurry for the same two experiments shown in Figure 8 (and their repeats). This result shows that the increase in the normalized pressure drop (flow loop ΔP with hydrates / ΔP without hydrates) is much more severe at the lower flow rate (300 rpm) than at the higher flow rate (550 rpm), or that at higher shear, a much greater volume fraction of hydrate in the slurry is required before a significant pressure drop increase is observed.
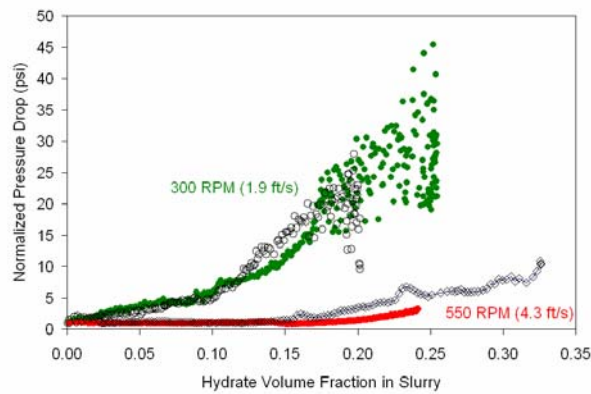
Figure 9. Flow loop pressure drop on hydrate formation with 300rpm pump speed, 35% water cut and Conroe crude oil (100% methane gas) – open symbols = repeat

Hydrate Transportability from Flow Loop Observations

The main two experimental variables that were found to effect hydrate flow loop transportability were: (1) the pump speed (or fluid velocity) and (2) the water cut. Higher pump speeds were found to help hydrate transportability. For the experiments at very low liquid volume fraction a greater hydrate volume fraction was required before a significant pressure drop was observed for the higher pump speed (550 rpm) compared with 300rpm. With the intermediate liquid loading and 50% water cut the highest pump speed (1400 rpm) produced a pumpable slurry, whereas the lower pump speed (900 rpm) resulted in the pressure drop exceeding the maximum allowed value.

The water cut also played an important role in determining the hydrate slurry transportability. The low water cut, 25%, formed hydrate without any transportability issues in the flow loop. For the highest water cut, 50%, the transportability was found to depend on the flow rate as discussed above. The intermediate water cuts (35% and 37.5%) showed signs of limited transportability. These were either an increase in pressure drop to erratic fluctuations as in the low liquid volume / low pump speed experiments, or the sharp increase in pressure drop to an eventual maximum safety shut-off pressure as in the intermediate liquid / high pump speed experiments.

The liquid volume fraction was also investigated but the limited results were inconclusive. The lowest liquid volume fraction experiments were limited to low pump speeds and the highest liquid volume fraction were limited to low water cuts.

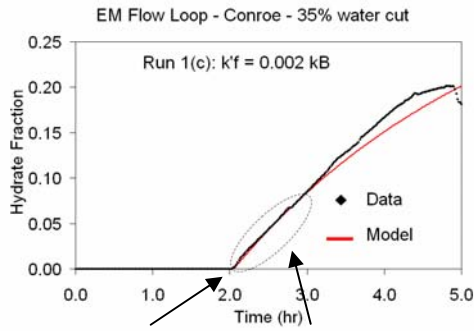**RESULTS – SIMULATION OF EXPERIMENTAL RESULTS**

A total of 15 flow loop experiments were modeled using CSMHyK-OLGA, as summarized in Table 2. Each run number is a combination of high (+) and low (-) independent variables.

Table 2. Experimental Matrix for ExxonMobil flow loop experiments, which were modeled.

| Ref:	ϕwc	ω	ϕg	P	η
Run1	+	–	–	–	–
Run2	+	+	–	–	–
Run5	–	–	–	–	–
Run6	–	+	–	–	–
Run11	+	–	–	+	–
Run12	+	+	–	+	–
Run13	+	–	–	+	+
Run14	+	+	–	+	+
Run15	+	–	–	–	+
Run16	+	+	–	–	+
Run21	–	–	–	+	–
Run22	–	+	–	+	–

Hydrate Formation Rate

In all simulations, the best fit rate constant was found by minimizing the difference between simulation and experiment for the first hour after nucleation. In most instances the data and the model followed reasonably closely after this first hour of formation. Hydrate nucleation time is an adjustable parameter in the model and the observed nucleation from the experiment was used as a simulation input. Figure 10 shows a comparison between the data and the model, with two fitted parameters: (1) – the hydrate nucleation point and (2) hydrate formation rate constant.

Figure 10. Comparing the flow loop experiment with the CSMHyK-OLGA simulation

The surface area for hydrate formation was found to be an important variable in the comparison between the experimental and simulated hydrate formation rate. To calculate the surface area, the assumption was made that the water was fully emulsified and that the droplets had a mean droplet diameter of 40 μm. The surface area was calculated using this assumption and the adjustment to the hydrate formation rate constant was fit to the data (Figure 11). From FBRM particle size measurements during the ExxonMobil flow loop experiments, 40 μm was found to be a reasonable mean droplet diameter as mean sizes ranged from 28-67 μm [6].
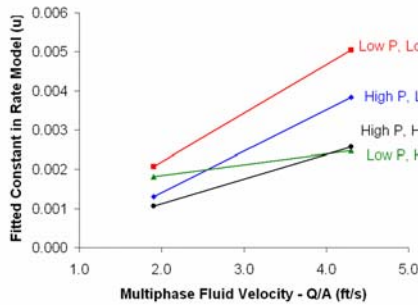
(a)
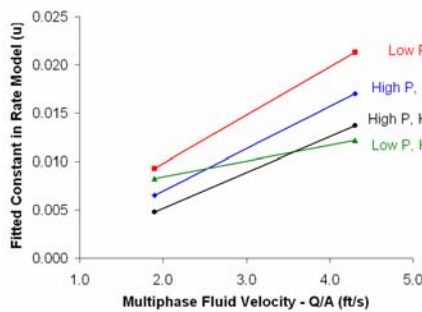
(b)

Figure 11. Fitted formation rate constants for the best fit with CSMHyK-OLGA simulations

The most significant trend observed for the fitted hydrate formation rate constant is the dependence on the multiphase flow velocity (pump speed). The formation rate constant increased with increasing velocity. One explanation for this trend is that the droplet size (assumed to be the same or 40 μm) would reduce with increasing shear (or velocity). The result of this would be an increased surface area for hydrate formation.

To test the dependence of the hydrate formation rate on the droplet size, the average hydrate formation rate constant from above (assuming a mean 40 μm diameter) was used ($k'_f = 0.002 \ k_B$), and the mean droplet diameter that best describes the surface area was fit to the data (Figure 12).
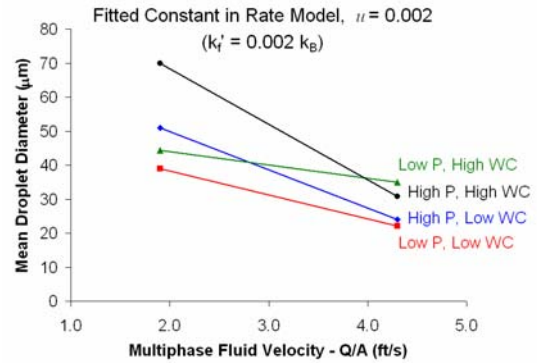

Figure 12. Fitted mean droplet diameters for the best fit with the CSMHyK-OLGA simulations

The resulting droplet sizes in Figure 12 fit nicely with the droplet sizes that were measured in the flow loop (given in Turner's thesis, 28-67 μm [6]).

The other trends that can be observed in the fitted formation rate constant for hydrate formation is that there seems to be a small dependence of the fitted constant on the water cut (Figure 11a) where a higher fitted constant is required for a lower water cut. Also a small dependence of the viscosity is observed (Figure 11b) where a higher fitted constant is required for the lower viscosity experiments.

The trends in the fitted constant in the rate model can generally be explained by hydrate formation in the flow loop experiments being limited by mass transfer to the hydrate reaction zone. The average required rate constant adjustment (for an assumed 40 μm mean droplet diameter) is 0.2% of the

"intrinsic" kinetic constant k_B, which suggests that hydrate formation is not limited by the kinetic reaction rate, but by either mass or heat transfer.

The temperature rise in the flow loops from the exothermic hydrate formation was not significant in most experiments, indicating that the heat transfer from the flow loop was not limiting the reaction, thus mass transfer of the hydrate formers (methane, and in some experiments methane + ethane) was likely the limiting factor. Three major trends in the variability of the fitted formation constant were observed and all three can be explained by limitations in the mass transfer.

The most significant trend is an increase in hydrate formation with fluid velocity (or pump speed). This can be explained by a combination of both increased surface area (from decreased droplet size) and also an increased diffusion in the oil phase due to the increased velocity. Two minor trends were an increase in the fitted constant with (1) decreased viscosity and (2) decreased water cut. The lower viscosity of the continuous oil phase would increase the diffusion of the dissolved gas hydrate formers and increase the mass transfer, resulting in an increase in the fitted rate constant. The lower water cut also decreases the effective viscosity of the emulsion, resulting in an increase in the fitted rate constant.

Although heat transfer does not appear to limit hydrate formation in the flow loop it may play an important role in larger diameter systems often seen in the field where the surface to volume ratio of pipeline is much lower. CSMHyK-OLGA simulations of a model tie-back system showed that heat transfer can control the hydrate formation when the heat removal from the pipe is insufficient to counteract the exothermic heat of formation. In this scenario the system temperature will quickly rise to the hydrate equilibrium temperature and the hydrate formation rate will thus be limited by the rate at which heat is removed from the flowing conduit. More information about this scenario can be found in an additional paper in the conference proceedings [7]

Hydrate formation flow loop experiments modeled using CSMHyK-OLGA have shown good agreement between the model and the data, but the greatly reduced formation rate constant suggests future efforts in modeling must incorporate both mass and heat transfer limitations to hydrate formation and cannot just be based upon intrinsic kinetics. This extension of the model is currently being performed at CSM.

CONCLUSIONS

Hydrate formation experiments have been carried out on a four inch flow loop to: (1) investigate the effect experimental variables have on the transportability of hydrate slurries and (2) investigate how hydrate formation experimental results compare with the hydrate kinetic model CSMHyK incorporated into the multiphase flow simulator OLGA.

The main two experimental variables that were found to effect hydrate flow loop transportability were (1) the pump speed (or fluid velocity) and (2) the water cut. Higher pump speeds were found to help hydrate transportability. The water cut also played an important role in determining the hydrate slurry transportability. The low water cut, formed hydrate without any transportability issues in the flow loop. For the highest water cut, the transportability was found to depend on the flow rate. The intermediate water cuts had limited transportability. The liquid volume fraction was also investigated, but the limited results were inconclusive.

The hydrate formation data from the flow loop experiments have been invaluable for the verification of the hydrate kinetics model CSMHyK. The comparison of the simulation results with flow loop experiments have shown that a narrow range of fitted formation rate constants (0.001 to 0.005) or an average value of 0.002 was able to achieve a reasonable fit for the hydrate formation. This reduced formation rate constant (a reduction of the formation rate measured for intrinsic kinetics) shows that hydrate formation in the flow loop is not limited by the intrinsic kinetic rate but most likely mass transfer of the hydrate formers.

REFERENCES

[1]Turner D. et al. *Development of a Hydrate Kinetic Model and It's Incorporation into the OLGA 2000® Transient Multiphase Flow Simulator.* 5th International Conference on Gas Hydrates, 4018, Trondheim, Norway, 2005, p1231-1240.

[2]Vysniauskas A. and Bishnoi P.R. *A Kinetic Study of Methane Hydrate Formation.* Chemical Engineering Science, Vol. 38, No 7, pp1061-1972, 1983.

[3]Matthews P.N., Notz P.K., Widener M.W. and Prukop G. *Flow Loop Experiments Determine Hydrate Plugging Tendencies in the Field. Gas* Hydrates: Challenges for the Future. NYAS Vol. 912, p330-338.

[4]Camargo R. and Palermo T. *Rheological Properties of Hydrate Suspensions in an Asphaltenic Crude Oil.* Proc. 4th Int. Conf. Gas Hydrates, 2002, pp880-885, Yokahama.

[5]Turner D. et al. *Development of a Hydrate Kinetic Model and It's Incorporation into the OLGA 2000® Transient Multiphase Flow Simulator.* 5th International Conference on Gas Hydrates, 4018, Trondheim, Norway, 2005, p1231-1240.

[6]Turner, D., *Clathrate hydrate formation in water-in-oil dispersions*, Ph.D. thesis, Colorado School of Mines, Golden, CO. 2005

[7]Kinnari, K. et al. *Hydrate Plug Formation Prediction Tool – An Increasing Need For Flow Assurance In The Oil Industry*, 6th International Conference on Gas Hydrates, Vancouver, Canada, 2008.